

Spontaneous time-reversal symmetry breaking for spinless fermions on a triangular lattice

O. Tieleman,¹ O. Dutta,¹ M. Lewenstein,^{1,2} and A. Eckardt^{1,3}

¹ICFO – Institut de Ciències Fotòniques, Parc Mediterrani de la Tecnologia, E-08860 Castelldefels, Spain

²ICREA – Institució Catalana de Recerca i Estudis Avançats, Lluís Companys 23, E-08010 Barcelona, Spain

³Max Planck Institute for the Physics of Complex Systems,
Noethnitzer Str. 38, D-01187 Dresden, Germany.

(Dated: May 5, 2022)

As a minimal fermionic model with kinetic frustration, we study a system of spinless fermions in the lowest band of a triangular lattice with nearest-neighbor repulsion. We find that the combination of interactions and kinetic frustration leads to spontaneous symmetry breaking in various ways. Time-reversal symmetry can be broken by two types of loop current patterns, a chiral one and one that breaks the translational lattice symmetry. Moreover, the translational symmetry can also be broken by a density wave forming a kagome pattern or by a Peierls-type trimerization characterized by enhanced correlations among the sites of certain triangular plaquettes (giving a plaquette-centered density wave). We map out the phase diagram as it results from leading-order Ginzburg-Landau mean-field theory. Several experimental realizations of the type of system under study are possible with ultracold atoms in optical lattices.

Geometric frustration in classical and quantum many-body systems is a source of intriguing phenomena like extensive ground-state entropies, topological order, and exotic emergent low-energy physics [1–5]. It is naturally encountered in systems of antiferromagnetically coupled localized magnetic moments, arranged in a non-bipartite (e.g. triangular) lattice geometry that prohibits the favored antiparallel orientation between all pairs of neighboring moments. Recently, geometric frustration has also been induced in the *kinetics* of a system of ultracold bosonic atoms on a triangular lattice by dynamically inverting the sign of the tunneling matrix elements [6, 7]. For weak interaction the system shows spontaneous time-reversal (TR) symmetry breaking, whereas strong interactions are conjectured to lead to spin-liquid-like quantum disordered behaviour.

Here we investigate a minimal *fermionic* model with kinetic frustration: spinless fermions on a triangular lattice, with nearest-neighbor interactions. It can be realized, e.g., with ultracold dipolar atoms or molecules in an optical lattice [8–10]. In this system kinetic frustration appears naturally as a consequence of Fermi statistics. Namely, for filling well above one half particle per site, the system is governed by the low-energy states of the fermionic holes whose kinetics is determined by the sign-inverted tunneling matrix elements. We find that (depending on the filling) two types of loop currents can spontaneously emerge at experimentally accessible temperatures (a chiral one and one that breaks translational symmetry). Thereby TR symmetry is broken neither as a consequence of coupling the kinetics to further degrees of freedom (such as spin or sublattice orbital freedom in the unit cell) nor in a process involving (quasi)long-range order in a continuous degree of freedom (i.e. Bose condensation). Typically at least one of these two themes is encountered when TR symmetry is broken in fermionic

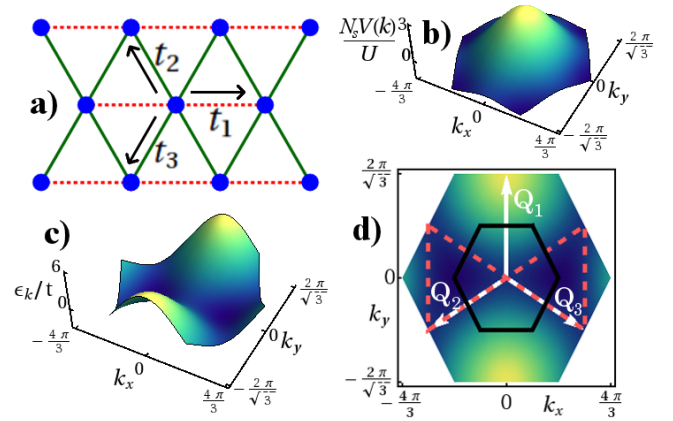


FIG. 1. (color online) (a) Frustrated triangular lattice, with solid (dashed) lines representing positive (negative) hopping parameters t_i ; the arrows indicate the vectors \mathbf{e}_i . (b) Momentum representation of the nearest neighbor interaction of strength U . (c) Single particle spectrum with two minima as a consequence of frustration. (d) First Brillouin zone with nested Fermi surface (dashed ‘bowtie’-shaped line) and nesting vectors (white arrows); the black line indicates the reduced Brillouin zone for 4-sublattice translational symmetry breaking.

systems; examples range from ferromagnetic metals to Mott-insulators with spin or orbital order, but comprise also exotic states like chiral spin liquids (not featuring Bose condensation) [11] or $p+ip$ superconductors (a condensate of pairs, not requiring spin) [12–15].

We also observe that the nesting property of the Fermi surface near hole filling of $1/4$ gives rise to a rich spectrum of three different types of instabilities that break the translational symmetry: One of them leads to spatially modulated currents (MC) and has been mentioned

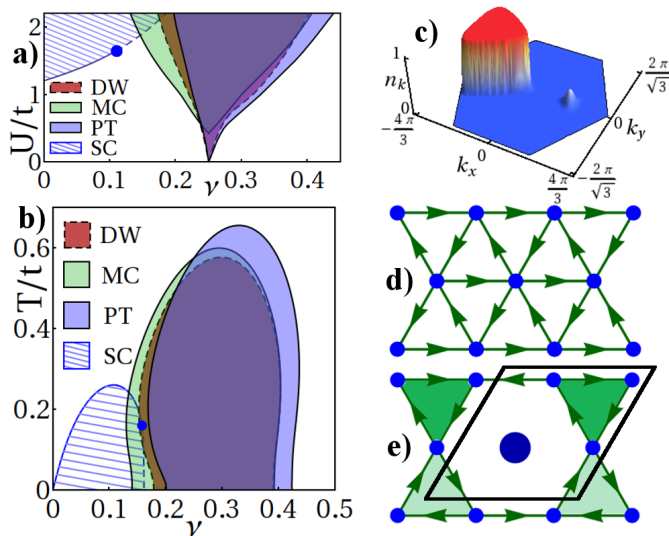


FIG. 2. (color online) (a) and (b) Phase diagram resulting from low-order Landau expansion of the mean-field free energy, with respect to interaction strength U/t , temperature T/t , and filling ν . Solid (dashed) lines indicate second (first) order transitions; $T/t = 0$ in a) and $U/t = 2$ in b). (c) Momentum density distribution example for SC phase. (d) Real-space pattern of staggered loop currents. (e) Three types of translational symmetry breaking with four-site unit cell (black line): Modulated currents (MC, arrows) defining a kagome lattice embedded into the triangular lattice, a density-wave (DW, larger dot represents increased site occupation), and Peierls-type trimerization [PT, triangular plaquettes with increased (lowered) correlations are indicated by dark (light) green shading].

already. The other two give rise to a density wave (DW) and to a Peierls-type trimerization (PT, a plaquette-centered density wave).

Model Our system is governed by the Hamiltonian

$$H = \sum_{\mathbf{r}} \sum_{\mathbf{r}'=\mathbf{r}\pm\mathbf{e}_i} \left(-t_i \hat{c}_{\mathbf{r}}^\dagger \hat{c}_{\mathbf{r}'} + \frac{U}{2} \hat{c}_{\mathbf{r}}^\dagger \hat{c}_{\mathbf{r}'}^\dagger \hat{c}_{\mathbf{r}'} \hat{c}_{\mathbf{r}} \right). \quad (1)$$

Here $\hat{c}_{\mathbf{r}}$ denotes the annihilation operator for a fermion at the lattice site located at \mathbf{r} , and the sum runs over all pairs of neighboring sites (connected by vectors $\pm\mathbf{e}_i$; see Fig. 1a). Interactions between different sites can be achieved in various ways, e.g. by using dipolar atoms or molecules that are polarized perpendicular to the lattice plane [9, 16–20] or as a superexchange process between neighboring sites in a mixed Mott insulator of fermions and bosons [21–24]. For simplicity, we have used isotropic nearest-neighbor interactions of strength $U > 0$ [25]. The tunneling matrix elements read $t_1 = -t$ and $t_2 = t_3 = t$ with $t > 0$ (see Fig. 1a), giving a π -flux through each plaquette. This sign configuration corresponds simply to studying holes instead of particles (which makes a difference in the non-bipartite triangular lattice) in a momentum shifted reference frame [26]. Another option is to

control the sign of the t_i via lattice shaking [6, 7]. The system of N particles on N_s sites (with filling $\nu = N/N_s$) is characterized, moreover, by the temperature T .

The tunneling coefficients are such that the kinetic energy cannot be minimized between all neighboring sites at the same time, since negative (positive) t_i favor a single particle state with a relative phase of π (0) between neighboring sites; the system is kinetically frustrated [6]. As a consequence, the single-particle dispersion relation $\varepsilon(\mathbf{k}) = -\sum_i 2t_i \cos(\mathbf{e}_i \cdot \mathbf{k})$ possesses two minima (see Fig. 1c). It is possible, however, to maximize the kinetic energy on every pair of neighboring sites, so the system is sensitive to the frustration for low filling only, when the Fermi surface explores low-energy states.

The double-well structure of the dispersion relation supports various interaction-driven instabilities. One of them results from interaction favoring particles to be close by in (quasi)momentum: The potential energy between two fermions with sharp momenta \mathbf{p} and $\mathbf{p}+\mathbf{q}$ reads $V(\mathbf{0}) - V(\mathbf{q}) \equiv \tilde{V}(\mathbf{q})$, where the Fourier transform of the interaction $V(\mathbf{q}) = N_s^{-1} \sum_i U \cos(\mathbf{e}_i \cdot \mathbf{q})$ decays with $|\mathbf{q}|$ (see Fig. 1b), and the relevant momentum-dependent second term (the exchange term) obtains a minus sign from Fermi statistics. For low filling this can, despite the kinetic energy cost, favor an imbalanced occupation of the two wells (see Fig. 2c) corresponding to staggered loop currents (SC) (see Fig. 2d).

Another source of instability appears near filling $\nu = 1/4$ where both minima are filled up. Here the Fermi surface forms a bow-tie (Fig. 1d, dashed line) and becomes approximately nested. Namely, $\varepsilon_{\mathbf{k}} - \varepsilon_{\mathbf{k}+\mathbf{Q}} \approx \varepsilon_F - \varepsilon_{\mathbf{k}+\mathbf{Q}}$ with Fermi energy ε_F and the same nesting vector \mathbf{Q} for a significant fraction of momenta \mathbf{k} near the Fermi surface, making the kinetic energy cost for spatial modulation described by \mathbf{Q} low [27] [28]. The nesting occurs for three vectors \mathbf{Q}_j (Fig. 1d, white arrows; \mathbf{Q}_j and $-\mathbf{Q}_j$ are equivalent since $2\mathbf{Q}_j$ is a reciprocal lattice vector). We find different instabilities that break translational symmetry (see Fig. 2e), to be described below.

The model (1) with nearest-neighbor repulsion has recently also been studied in the strong coupling limit $U/t \gg 1$, where for intermediate filling ($1/3 \leq \nu \leq 2/3$) frustrated interactions lead to DW order [29–31]. In contrast, we are approaching the problem from the weak-coupling (mean-field) regime at low filling ($\nu \lesssim 1/4$) and find TR symmetry breaking as a consequence of frustrated kinetics. Fermions on the kagome lattice have been investigated in Refs. [32, 33].

Method We use mean-field theory as a first approach (see Refs. [34, 35] for the square lattice). In momentum representation, $\hat{a}_{\mathbf{k}} = N_s^{-1/2} \sum_{\mathbf{r}} e^{-i\mathbf{k}\cdot\mathbf{r}} \hat{c}_{\mathbf{r}}$, the interaction consists of terms $V(\mathbf{q}) \hat{a}_{\mathbf{k}+\mathbf{q}}^\dagger \hat{a}_{\mathbf{p}-\mathbf{q}}^\dagger \hat{a}_{\mathbf{p}} \hat{a}_{\mathbf{k}}$ that we approximate like $\hat{a}_{\mathbf{k}}^\dagger \hat{a}_{\mathbf{l}}^\dagger \hat{a}_{\mathbf{p}} \hat{a}_{\mathbf{q}} \approx \xi_{\mathbf{k}\mathbf{q}} \hat{a}_{\mathbf{l}}^\dagger \hat{a}_{\mathbf{p}} + \xi_{\mathbf{l}\mathbf{p}} \hat{a}_{\mathbf{l}}^\dagger \hat{a}_{\mathbf{q}} - \xi_{\mathbf{k}\mathbf{q}} \xi_{\mathbf{l}\mathbf{p}} - \xi_{\mathbf{k}\mathbf{p}} \hat{a}_{\mathbf{l}}^\dagger \hat{a}_{\mathbf{q}} - \xi_{\mathbf{l}\mathbf{q}} \hat{a}_{\mathbf{k}}^\dagger \hat{a}_{\mathbf{p}} + \xi_{\mathbf{k}\mathbf{p}} \xi_{\mathbf{l}\mathbf{q}}$ while asking for self-consistency $\xi_{\mathbf{k}\mathbf{p}} = \langle \hat{a}_{\mathbf{k}}^\dagger \hat{a}_{\mathbf{p}} \rangle$. Allowing for spatial modulations

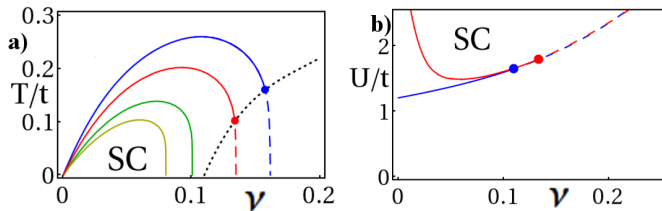


FIG. 3. (color online) Phase boundary of parameter region where staggered currents are expected (from low-order Landau expansion of the mean-field free energy) Solid (dashed) lines indicate second (first) order transitions. (a) $U/t = 1.5, 1.6, 1.8, 2$, from small to large regions. (b) $T/t = 0$ (blue, crossing y -axis) and $T/t = 0.2$ (red, not crossing y -axis).

described by the nesting vectors, we retain averages of the form $\langle \hat{a}_{\mathbf{k}-\mathbf{Q}_j}^\dagger \hat{a}_{\mathbf{k}} \rangle$ with $j = 0, 1, 2, 3$ where $\mathbf{Q}_0 \equiv \mathbf{0}$. Accordingly, we have single-particle correlations

$$\langle \hat{c}_{\mathbf{r}+\mathbf{e}_i}^\dagger \hat{c}_{\mathbf{r}} \rangle = \sum_{j=0}^3 e^{i\mathbf{r}\cdot\mathbf{Q}_j} c_{ij} \quad (2)$$

where $c_{ij} = N_s^{-1} \sum_{\mathbf{p}} e^{-i(\mathbf{p}-\mathbf{Q}_j)\cdot\mathbf{e}_i} \langle \hat{a}_{\mathbf{p}-\mathbf{Q}_j}^\dagger \hat{a}_{\mathbf{p}} \rangle$ (summing over one Brillouin zone). Defining $\mathbf{e}_0 = \mathbf{0}$, the local density $n_{\mathbf{r}} = \langle \hat{c}_{\mathbf{r}}^\dagger \hat{c}_{\mathbf{r}} \rangle$ is related to the four averages $c_{0j} \equiv \rho_j$. The current from \mathbf{r} to $\mathbf{r} + \mathbf{e}_i$, namely $J_i(\mathbf{r}) = 2t_i \text{Im} \langle \hat{c}_{\mathbf{r}+\mathbf{e}_i}^\dagger \hat{c}_{\mathbf{r}} \rangle / \hbar$, is described by $\text{Im} c_{ij} \equiv I_{ij}$ ($i \neq 0$, using the equivalence of \mathbf{Q}_j and $-\mathbf{Q}_j$). We also define $\text{Re} c_{i \neq 0j} \equiv R_{ij}$ for the real (non-current-generating) part of the correlations $\langle \hat{c}_{\mathbf{r}+\mathbf{e}_i}^\dagger \hat{c}_{\mathbf{r}} \rangle$. The terms $\rho_0 = N/N_s$ and R_{i0} are non-zero already without symmetry breaking.

Staggered currents Well below quarter filling, nesting is irrelevant and only terms with $j = 0$ are important. The free energy reads

$$F = -T \sum_{\mathbf{k}} \ln(1 + e^{-\omega_{\mathbf{k}}/T}) - \sum_{\mathbf{p}, \mathbf{q}} \tilde{V}(\mathbf{p} - \mathbf{q}) n_{\mathbf{p}} n_{\mathbf{q}}, \quad (3)$$

with $n_{\mathbf{k}} \equiv \langle \hat{a}_{\mathbf{k}}^\dagger \hat{a}_{\mathbf{k}} \rangle$ and mean-field dispersion relation $\omega_{\mathbf{k}} = 2 \sum_{i=1}^3 [(t_i + UR_{i0}) \cos(\mathbf{k} \cdot \mathbf{e}_i) + UI_{i0} \sin(\mathbf{k} \cdot \mathbf{e}_i)]$. If F is minimal for finite momentum imbalances $I_{i0} = N_s^{-1} \sum_{\mathbf{p}} \sin(\mathbf{p} \cdot \mathbf{e}_i) n_{\mathbf{p}}$, loop currents will emerge.

In order to learn when this happens, we apply perturbation theory within the imaginary time formalism and Landau expand the free energy in powers of the I_{i0} :

$$F \simeq F_0 + \mathbf{I}_1^T M \mathbf{I}_1 + \mathbf{I}_2^T K \mathbf{I}_2 + \mathcal{O}(I_{i0}^6). \quad (4)$$

Here $\mathbf{I}_n^T = (I_{10}^n, I_{20}^n, I_{30}^n)$ (with power n and transposition T), F_0 is a constant, and M and K are symmetric matrices. A second-order transition into a phase with finite $\mathbf{I}_1^T = (-1, 1, 1)I$ occurs when m_2 , the lowest eigenvalue of M , becomes negative, while higher-order contributions to F remain positive. The resulting phase boundaries are plotted as solid lines in Fig. 3.

If the quartic term, with matrix elements $K_{ij} = \delta_{ij}|\eta| + (1 - \delta_{ij})\zeta$, becomes negative for $2\zeta < -|\eta|$ on the line defined by $m_2 = 0$, the phase transition becomes first-order (indicated by dashed lines in Fig. 3) and the boundary shifts away from $m_2 = 0$, enlarging the symmetry broken region (neglected in Fig. 3). Minimising the free energy (3) beyond the Landau expansion (4) we find this shift to be small.

The current pattern in the symmetry-broken phase is defined by $J_i(\mathbf{r}) = J$, giving a staggered pattern of circular plaquette currents as shown in Fig. 2d. The state is two-fold degenerate ($J = \pm|J|$) and chiral in the sense that both TR and lattice inversion transform one solution into the other [11]. Experimentally this state can be identified by the momentum imbalance visible in time-of-flight absorption images.

The phase diagram (Fig. 3) can be understood as follows. For lower densities, the slope of the single-particle spectrum at the Fermi surface is flatter (see Fig. 1c), which explains why the critical interaction strength is reduced when the filling is lowered. If the filling is too low, however, a finite temperature T may overcome the energy scale $U\nu$ of the interaction and destroy the currents altogether. Increasing the temperature counteracts the clustering effect from momentum-space attraction and makes symmetry breaking less favorable.

For low filling $\nu < 1/3$ no competing symmetry broken state is expected in the strong-coupling limit $U/t \gg 1$ [29–31]. This makes it likely that the SC phase is not destroyed by quantum fluctuations beyond mean-field. We have performed exact diagonalizations for a small system (3 particles on 45 sites) at $T = 0$, and find an increased admixture to the ground state of kinetic energy eigenstates with large $|I_{i0}|$ for $U/t \gtrsim 1$, in support of the mean-field findings.

Spatial modulation Near quarter filling, where nesting becomes relevant, we have to take into account the additional possibility of spatial modulation described by the nesting vectors. This leads to a triangular lattice with four-site unit cell (see Fig. 2e), such that the mean-field Hamiltonian possesses four bands in a reduced Brillouin zone (see Fig. 1d). Broken translational symmetry is indicated by finite averages ρ_j , R_{ij} , or I_{ij} , with $j \neq 0$, that open a gap between the lowest bands [36]. Expanding the free energy also with respect to those averages, in the leading (quadratic) order we find

$$F_{\text{mod}}^{(2)} = \sum_{j=1}^3 \left[\mathbf{D}_j^T A \mathbf{D}_j + \mathbf{R}_j^T B \mathbf{R}_j + \mathbf{J}_j^T C \mathbf{J}_j + \lambda I_{jj}^2 \right] \quad (5)$$

with vectors $\mathbf{D}_j^T = (\rho_j, R_{jj})$, $\mathbf{R}_j^T = (R_{kj}, R_{lj})$ and $\mathbf{J}_j^T = (I_{k,j}, I_{l,j})$ such that $j \rightarrow k \rightarrow l$ under cyclic permutation, symmetric 2×2 matrices A , B and C , and coefficient $\lambda > 0$. Thus $I_{jj} = 0$ is favored. The remaining averages are coupled pairwise, with different nesting directions j uncoupled in quadratic order.

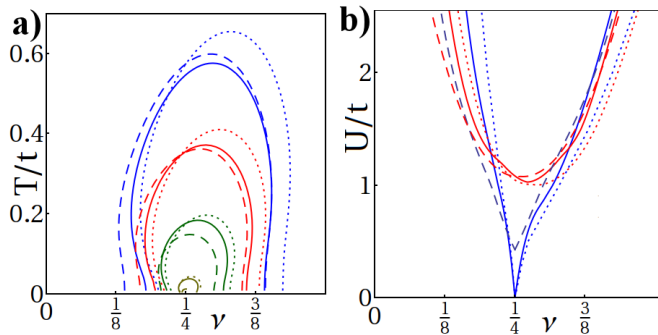


FIG. 4. (color online) Different types of instabilities that break the translational lattice symmetry are found inside the plotted boundaries. Solid, dotted, and dashed lines stand for instabilities leading to density-wave order, Peierls-type trimerization (i.e. plaquette-centered density-wave order), and a pattern of modulated currents, respectively. The transition to the density-wave order has to be first order. (a) $U/t = 0.5$ (inner curve), 1, 1.5, 2 (outer curves), (b) $T/t = 0$ (lower curves) and 0.1 (upper curves).

A DW instability appears when the lowest eigenvalue of A becomes negative (solid boundaries in Fig. 4). In third order we find a term $\Gamma \rho_1 \rho_2 \rho_3$ that couples the density modulations along the three directions j . It favors the four-fold degenerate DW pattern shown in Fig. 2e with the low-density sites defining a kagome lattice (and the coupling to R_{jj} reducing the correlations among the low-density sites). The third-order term also renders the transition first order and shifts the phase boundary slightly (neglected in Fig. 4). Exact diagonalization studies with 4 particles on 16 sites at $T = 0$ confirm kagome DW patterns (with a slight anisotropy, probably a finite-size effect).

If the lowest eigenvalue of B turns negative (Fig. 4, dotted lines), an instability towards a Peierls-type modulation of nearest-neighbor correlations is found: The correlations $\langle \hat{c}_r^\dagger, \hat{c}_r \rangle$ on the dark (light) shaded triangular plaquettes in Fig. 2e are increased (lowered); or vice versa. This eight-fold degenerate Peierls trimerization breaks also the inversion symmetry of the lattice and corresponds to a plaquette-centered DW.

Finally, if C acquires a negative eigenvalue (Fig. 4, dashed lines) an instability towards the formation of MC is indicated. The current carrying bonds define a kagome lattice with loop currents of equal orientation around both types of triangular plaquettes (\triangle and ∇) and of opposite orientation around the hexagonal plaquettes (see Fig. 2e), such that the finite plaquette fluxes of the mean-field Hamiltonian vanish when averaged over the unit cell. This pattern breaks both TR and translational symmetry and is eight-fold degenerate.

The structure of the stability boundaries shown in Fig. 4 explains itself in an intuitive way. According to

the nesting condition, interaction-induced spontaneous translational symmetry breaking occurs for filling near $1/4$, in a finite interval of filling factors that grows with increasing interactions. An interesting effect is that for a given interaction strength U/t this interval has its maximum extent at a non-zero temperature. The growth of the symmetry broken parameter region when a small temperature is switched on, might be explained by the fact that smoothening the Fermi edge increases the number of participating momentum pairs for which the nesting condition is approximately fulfilled. However, for large temperatures the order is eventually destroyed.

As visible in Figure 4 there is a large region in parameter space, where according to second Landau order all three nesting-driven types of symmetry breaking instabilities appear. As long as the spontaneous kagome patterns defined by each of them match (as depicted in Fig. 2e), they can in principle co-exist; their structures do not mutually exclude each other. This suggests that (especially as long as the order parameters are small such that low-order Landau terms dominate) the system might take advantage of realizing two or even all three of them at the same time, leading to a degeneracy of up to sixteen ($4 \times$ spatial, $2 \times$ time-reversal, and $2 \times$ inversion symmetry). However, generally it will depend on the energetics described by higher-order Landau terms that contain the coupling between the different orders, whether mean-field theory predicts such co-existences. Shifting and merging of the phase boundaries due to higher-order terms can be expected. Beyond mean-field theory this question can be answered, for example, by an experiment with ultracold atoms.

All three translational symmetry breaking orders (DW, MC, and PT) open up a gap between the lowest two bands of the mean-field dispersion relation in the reduced Brillouin zone. However, the momentum-space structure of the coupling that induces the gap depends on the type of order. Thus the three orders can be distinguished by the momentum distribution, which is accessible through time-of-flight absorption imaging. The orders involving loop currents could, moreover, be observed using a quench in the tunnelling matrix elements [37, 38]. Exactly at quarter (hole) filling, an insulating phase is expected due to the gap, which should show up as a plateau (at particle filling $3/4$) in the density profile in a shallow trap.

We summarize our findings in Fig. 2 with subfigures (a) and (b) showing the combined phase diagram. For sufficiently large interactions there is a small parameter region where both the SC and the MC overlap. We expect both types of order to repel each other and it appears likely that higher order terms will remove this overlap region and predict a direct transition between both phases.

We conclude that kinetic frustration, as it emerges naturally in a non-bipartite lattice potential at low filling of

fermionic holes, can give rise to rich physics without involving spin degrees of freedom. We find that for spinless fermions on a triangular lattice with nearest neighbor repulsion it gives rise to a number of interesting symmetry broken phases. They are characterized by chiral or modulated loop currents, Peierls-type trimerisation, and density-wave order. Our findings can be probed experimentally with ultracold fermionic atoms or molecules in optical lattices at accessible temperatures. Such an experiment would complement the recent observation of time-reversal symmetry breaking as a consequence of kinetic frustration in a system of bosonic atoms [7]. Many fascinating questions related to the findings discussed here can be investigated, including the role of quantum fluctuations beyond mean field, and such natural generalizations as the inclusion of a second spin species and on-site interactions. We hope to inspire such research with this paper.

ACKNOWLEDGEMENTS

OT thanks Achilleas Lazarides for helpful discussions and acknowledges funding from the Netherlands Organization for Scientific Research (NWO). Furthermore, we acknowledge funding from AAII-Hubbard, EU STREP NAMEQUAM, ERC AdG QUAGATUA, Humboldt Stiftung, Joachim Herz Stiftung, University of Hamburg and the foundation universidad.es.

-
- [1] X.-G. Wen, *Quantum Field Theory of Many-Body Systems* (Oxford University Press, New York, 2004).
- [2] C. Lhuillier, arXiv:cond-mat/0502464 (2005).
- [3] F. Alet, A. M. Walczak, and M. P. A. Fisher, *Physica A* **369**, 122 (2006).
- [4] R. Moessner and A. P. Ramirez, *Physics Today* **59-2**, 24 (2006).
- [5] S. Sachdev, *Nucl. Phys.* **4**, 173 (2008).
- [6] A. Eckardt, P. Hauke, P. Soltan-Panahi, C. Becker, K. Sengstock, and M. Lewenstein, *EPL* **89**, 10010 (2010).
- [7] J. Struck, C. Ölschläger, R. L. Targat, P. Soltan-Panahi, A. Eckardt, M. Lewenstein, P. Windpassinger, and K. Sengstock, *Science* **333**, 996 (2011).
- [8] M. Lewenstein, A. Sanpera, and V. Ahufinger, *Ultracold Atoms in Optical Lattices: Simulating quantum many-body systems* (Oxford University Press, Oxford, UK, 2012).
- [9] T. Lahaye, C. Menotti, L. Santos, M. Lewenstein, and T. Pfau, *Rep. Prog. Phys.* **72**, 126401 (2009).
- [10] I. Bloch, J. Dalibard, and W. Zwerger, *Rev. Mod. Phys.* **80**, 885 (2008).
- [11] X. G. Wen, F. Wilczek, and A. Zee, *Phys. Rev. B* **39**, 11413 (1989).
- [12] W. Kohn and J. M. Luttinger, *Phys. Rev. Lett.* **15**, 524 (1965).
- [13] G. Volovik, *JETP Letters* **70**, 609 (1999), 10.1134/1.568223.
- [14] N. Read and D. Green, *Phys. Rev. B* **61**, 10267 (2000).
- [15] D. A. Ivanov, *Phys. Rev. Lett.* **86**, 268 (2001).
- [16] A. Griesmaier, J. Werner, S. Hensler, J. Stuhler, and T. Pfau, *Phys. Rev. Lett.* **94**, 160401 (2005).
- [17] C. Trefzger, C. Menotti, B. Capogrosso-Sansone, and M. Lewenstein, *J. Phys. B* **44**, 193001 (2011).
- [18] M. Lu, N. Q. Burdick, and B. L. Lev, *Phys. Rev. Lett.* **108**, 215301 (2012).
- [19] K. K. Ni, S. Ospelkaus, D. Wang, G. Quemener, B. Neyenhuis, M. H. G. de Miranda, J. L. Bohn, J. Ye, and D. S. Jin, *Nature* **464**, 13241328 (2010).
- [20] C.-H. Wu, J.W. Park, P. Ahmadi, S. Will, and M.W. Zwierlein, *Phys. Rev. Lett.* **109**, 085301 (2012).
- [21] A. B. Kuklov and B. V. Svistunov, *Phys. Rev. Lett.* **90**, 100401 (2003).
- [22] M. Lewenstein, L. Santos, M.A. Baranov, and H. Fehrmann, *Phys. Rev. Lett.* **92**, 050401 (2004).
- [23] A. Eckardt and M. Lewenstein, *Phys. Rev. A* **82**, 011606(R) (2010).
- [24] S. Sugawa, K. Inaba, S. Taie, R. Yamazaki, M. Yamashita, and Y. Takahashi, *Nature Phys.* **7** (2011).
- [25] In the case of dipolar interactions, the restriction to nearest-neighbor constitutes an approximation. However, we expect that including longer-range terms the mean-field theory would yield qualitatively similar results, since both momentum-space attraction and nesting (described below) would still be present.
- [26] Starting from the standard (zero flux) configuration for particles, $t_i > 0$, a particle-hole transformation $\hat{c}_r \rightarrow \hat{c}_r^\dagger$, implying $\hat{n}_r = \hat{c}_r^\dagger \hat{c}_r \rightarrow 1 - \hat{n}_r$, inverts all tunneling matrix elements, $t_i \rightarrow -t_i$, while it leaves the interaction term (up to a constant) unchanged. We find it convenient to apply another transformation $\hat{c}_r \rightarrow \exp(i\mathbf{q} \cdot \mathbf{r}) \hat{c}_r$ [describing a shift in quasimomentum by $\mathbf{q} = (0, 2\pi/\sqrt{3})$] that inverts back t_2 and t_3 .
- [27] T. M. Rice and G. K. Scott, *Phys. Rev. Lett.* **35**, 120 (1975).
- [28] The nesting is not exact because the condition only holds approximately, near the Fermi surface.
- [29] C. Hotta and N. Furukawa, *Phys. Rev. B* **74**, 193107 (2006).
- [30] C. Hotta, N. Furukawa, A. Nakagawa, and K. Kubo, *J. Phys. Soc. Jpn.* **75**, 123704 (2006).
- [31] S. Nishimoto and C. Hotta, *Phys. Rev. B* **79**, 195124 (2009).
- [32] A. O'Brien, F. Pollmann, and P. Fulde, *Phys. Rev. B* **81**, 235115 (2010).
- [33] M. L. Kiesel, C. Platt, and R. Thomale, arXiv:1209.3398 (2012).
- [34] K. Mielson and J.K. Freericks, *Phys. Rev. A* **83**, 043609 (2011).
- [35] E. Halvorsen, G. S. Uhrig, and G. Czycholl, *Z. Phys. B* **94**, 291 (1994).
- [36] The gap opens along the $\nu = 1/4$ -Fermi surface, forming a star-shaped structure in the reduced Brillouin zone.
- [37] M. Killi and A. Paramekanti, *Phys. Rev. A* **85**, 061606(R) (2012).
- [38] M. Killi, S. Trotzky, and A. Paramekanti, arXiv:1210.4554 (2012).